Chronobiology International, 26(8): 1514–1544, (2009)

ISSN 0742-0528 print/1525-6073 online
DOI: 10.3109/07420520903553435

informa
healthcare

RESEARCH PAPERS

EXPRESSION PROFILING REVEALS A POSITIVE REGULATION BY *MPER2* ON CIRCADIAN RHYTHM OF CYTOTOXICITY RECEPTORS: *LY49C* AND *NKG2D*

Yonglun Luo,[1,3] Weiping Tian,[1] Lun Cai,[2] Yan Wang,[1] Jing Zhang,[1] Huajing Teng,[1] Jie Du,[1,2] and Zhong Sheng Sun[1,3]

[1]*Behavioral Genetics Center, Institute of Psychology, Chinese Academy of Sciences, Beijing, China*
[2]*Beijing Anzhen Hospital affiliated to Capital Medical University, Beijing Institute of Heart Lung and Blood Vessel Diseases, Beijing, China*
[3]*Graduate University of the Chinese Academy of Sciences, Beijing, China*

The mammalian circadian gene, *mPer2*, an indispensable component of the mammalian circadian clock, not only modulates endogenous circadian rhythms but also plays a crucial role in regulating innate immune function. Previously, we showed that *mPer2* plays a crucial role in regulating cytotoxic response. To investigate the molecular mechanism for *mPer2*-controlled cytotoxic response, in the present study we conducted mRNA expression for 11 genes participating in cytotoxicity regulation in wild-type (WT) and *mPer2* knockout ($mPer2^{-/-}$) mice bone marrow, that is, *Dap-10*, *Ly49C*, *Ly49I*, *Rac1*, *Mapk1*, *Map2k1*, *Nkg2d*, *Shp-1*, *Pak1*, *Pik3ca*, and *Vav1*. The mRNA levels of *Ly49C* ($p < 0.001$), *Ly49I* ($p = 0.039$), and *Nkg2d* ($p = 0.038$) were significantly downregulated in $mPer2^{-/-}$ mice. Time-dependence of expression profiling was then conducted for four core clock genes (*Per1*, *Bmal1*, *Clock*, *Rev-erbα*), and six out of these 11 cytotoxic regulation genes (*Ly49C*, *Ly49I*, *Mapk1*, *Nkg2d*, *Shp-1*, *Pik3ca*) in WT and $mPer2^{-/-}$ entrained in light/dark (LD) or dark/dark (DD) cycles. Consistently, circadian oscillations were observed for *Per1*, *Rev-erbα*, *Ly49C*, and *Nkg2d* in WT mice under LD and DD cycles. However, these rhythmic expressions were either disrupted or dampened in $mPer2^{-/-}$ mice. Comparison of gene expression between WT and $mPer2^{-/-}$ mice showed that *mPer2* knockout had systematically downregulated the mRNA expression of two cytotoxicity regulators, *Ly49C* and *Nkg2d*. FACS analysis further confirmed that the circadian expression of these genes was not due to the daily difference in cell numbers of NK, NKT, or T cells in bone marrow. Taken together, our results reveal that *mPer2* is a critical clock component in modulating circadian rhythms in bone marrow. Furthermore, it implies that *Ly49C* and *Nkg2d* are two clock-controlled genes that may play an important role

Submitted April 10, 2009, Returned for revision May 5, 2009, Accepted July 15, 2009
Address correspondence to Dr. Zhong Sheng Sun, Behavioral Genetics Center, Institute of Psychology, Chinese Academy of Sciences, Beijing 101300, China; Tel.: 010-64840367; Fax: 010-64841050; E-mail: zsunusa@yahoo.com

in mediating *mPer2*-controlled cytotoxic response. (Author correspondence: zsunusa@yahoo.com)

Keywords Cytotoxicity regulation, Cytotoxicity receptors, *mPer2*, *Ly49C*, *Nkg2d*

INTRODUCTION

The circadian rhythms observed in multiple biological processes are driven by endogenous molecular clocks, which consist of a master clock residing in the suprachiasmatic nucleus (SCN) and slave clocks residing in peripheral tissues, such as heart, liver, spleen, adrenal gland, and bone marrow (Albrecht et al., 1997; Liu et al., 2007). This molecular circadian regulation of biological processes is organized in a positive-negative transcriptional-translational feedback loop, consisting of many clock components (Reppert et al., 2002). The positive limb of this feedback loop is formed by a pair of transcription factors, BMAL1 and CLOCK. BMAL1 and CLOCK form heterodimers and initiate the expression of *Period* (*Per1/2/3*) and *Cryptochrome* (*Cry1/2*). In contrast, PER and CRY form heterodimers and repress their own expression by interacting with the BMAL1:CLOCK complex, thereby forming a transcriptional and translational feedback loop. A more detailed description of this feedback loop is available elsewhere (Dardente & Cermakian, 2007; Ko et al., 2006).

Recent studies consistently indicate that *mPer2* not only acts as an indispensable component in modulating the endogenous circadian clock, but also plays a crucial role in regulating innate immune functions. Rhythmic expression of *mPer2* is present in bone marrow (Chen et al., 2000), peripheral blood mononuclear cells (Boivin et al., 2003; James et al., 2007), NK cells (Arjona et al., 2005), endocrine tissues (Bittman et al., 2003), and other immune organs (Liu et al., 2007). In addition, functional investigations had proven that *mPer2* plays an important role in tumor suppression, IFN-γ release regulation, cell apoptosis, and natural killer (NK) cell functions (Arjona et al., 2006; Fu et al., 2002; Liu et al., 2006). Mice deficient in the *mPer2* gene were genetically deficient in NK cell functions and cancer prone (Fu et al., 2002). Investigations conducted by other groups and us consistently demonstrate that daily rhythmic expression of IFN-γ as well as its induction to lipopolysaccharide-induced endotoxic shock are regulated by *mPer2* (Arjona et al., 2006; Liu et al., 2006).

It is well known that IFN-γ is a pre-inflammation cytokine released from endotoxic response. This cytokine plays an important role in mediating host responses to infection and tumors (Sasaki et al., 2006; Wall et al., 2003). IFN-γ production in an innate immune response is primarily rendered by NK, NKT, and T cells after stimulation by microbial

infection. Briefly, activation of the cytotoxicity pathway is achieved by activation of the transmembrane receptor NKG2D (Jamieson et al., 2002). Then, NKG2D interacts with DAP-10, which directly activates phosphatidylinositol 3-kinase (Pik3ca) and the MAPK signaling pathway (Billadeau et al., 2003). Thus NKG2D is a key molecular component in the stimulation of NK cells, CD8(+) T cells, and macrophage functions and plays a substantial role in natural killing. In contrast, the killer cell lectin-like receptors (Ly49C and Ly49I), which reside in the cell membrane of NK cells, T cells, and macrophages, are the crucial components in mediating inhibition of the natural killing process (Dimasi et al., 2005). Ly49 receptor engagement interacts with small heterodimer partners (SHP-1, SHP-2), a member of the nuclear receptor superfamily, and represses VAV1 activity, which leads to the suppression of cytotoxicity and IFN-γ production. It is well known that VAV1 controls DAP10-mediated natural cytotoxicity (Graham et al., 2006). Still, the underlying mechanisms governing daily oscillations of IFN-γ expression as well as endotoxic response by mPer2 are largely unknown. Furthermore, lower serum IFN-γ levels had been observed in *mPer2*$^{-/-}$ mice (Arjona et al., 2006; Liu et al., 2006). These findings probably indicate that IFN-γ production in *mPer2*$^{-/-}$ mice is genetically and developmentally deficient.

Consequently, our aim was to investigate which components of the cytotoxicity regulation process are likely to be involved in *mPer2*-controlled cytotoxic response and thus IFN-γ production regulation. For this purpose, expression changes of 11 genes (viz., *Dap-10*, *Ly49C*, *Ly49I*, *Rac1*, *Mapk1*, *Map2k1*, *Nkg2d*, *Shp-1*, *Pak1*, *Pik3ca*, and *Vav1*) involved in cytotoxicity and IFN-γ production, and four core clock genes (viz., *mPer1*, *mBmal1*, *mClock*, and *mRev-erbα*) were measured in the bone marrow of WT and *mPer2*$^{-/-}$ mice. Bone marrow is the origin of immune cell progenitors, such as the T/B lymphocyte, NK cell, and macrophage progenitors. The first indication of an endogenous molecular clock system in bone marrow was reported by Yi-Guang Chen and colleagues (2000), who found that *mPer1* and *mPer2* oscillated over a 24 h period in murine bone marrow. Oleg Tsinkalovsky and colleagues (2006) found that *Per2* and *Rev-erbα* display circadian rhythms in bone marrow, suggesting that *Per2* may play a very important role in regulating circadian physiology in bone marrow (Mendez-Ferrer et al., 2008).

In this report, we show that expressions of *Ly49C*, *Ly49I*, and *Nkg2d* are significantly downregulated in *mPer2*$^{-/-}$ mice bone marrow. Investigation of daily mRNA expression profiling shows *Ly49C* and *Nkg2d* oscillates over the 24 h period under both LD and DD cycles in WT mice bone marrow, while these rhythms are disrupted in *mPer2*$^{-/-}$ mice. Consistent with previous reports, *Per1* and *Rev-erbα* exhibits circadian oscillations in WT mice bone marrow (Granda et al., 2005; Tsinkalovsky

et al., 2006). Our data suggest that the circadian gene *mPer2* plays an important role in regulating bone marrow function, and that the definition of this role provides insight into the molecular mechanism for *mPer2* regulation of cytotoxic response. To the best of our knowledge, this is the very first report of circadian oscillations of *Ly49C* and *Nkg2d* in bone marrow, as well as the positive transcriptional regulation by *mPer2*. However, further experiments are needed to determine the detail regulation of *mPer2* on *Ly49C* and *Nkg2d*.

MATERIALS AND METHODS

Animals

Eight-week-old C57 BL/6 (purchased from the Animal Center of the Department of Animal Science of Peking University, Beijing, China) and *mPer2*$^{-/-}$ mice (bred in the Animal Facility of the Behavioral Genetics Center, CAS) were housed under a 12 h/12 h light/dark (LD) cycle with light on at 06:00 h (defined as Zeitgeber time 0, i.e., ZT0) and dark/dark (DD) cycle. They were housed individually in a running-wheel facility with food and water ad libitum. Experiments were conducted according to the principles and standards of the Chinese Academy of Science and met the ethical standards of the journal (Portaluppi et al., 2008).

Entrainment to Light/Dark (LD) Cycles and Dark/Dark (DD) Cycles in Wheel-Running Facility

In order to precisely determine the internal circadian time in DD, mice were entrained individually in a wheel-running cage equipped with a steel running wheel. The locomotor activity of the mice was recorded in real time using a magnetic switch and VitalView data monitor system (Mini Metter, USA). Light, noise, temperature, and humidity were maintained under suitable and stable conditions in an isolated, soundproof, and air-conditioned room. For LD cycles (zeitgeber time), mice were entrained in the wheel-running cage for two weeks with lights-on from 06:00 to 18:00 h. Mice were then sacrificed at the indicated timepoints. For DD (circadian time, free-running), mice were first entrained in 12 h/12 h LD for two weeks and then shifted into DD for 10 days, after which the mice were sacrificed and examined. CT12 was defined as the onset of the active phase. All period lengths were calculated according to previously reported methods (Jud et al., 2005). Because the locomotor activity of *mPer2*$^{-/-}$ mice was completely disrupted by being shifted into free-running (see Figure 1), the circadian timepoints of *mPer2*$^{-/-}$ mice were determined in accordance with that in WT mice.

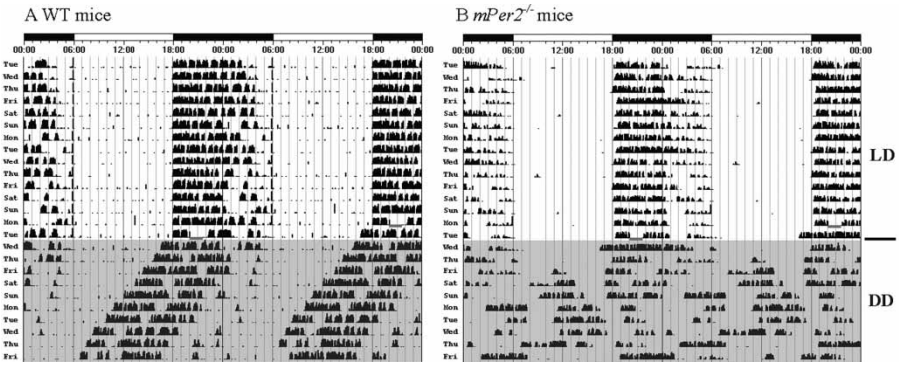

FIGURE 1 Actograms of WT and $mPer2^{-/-}$ mice locomotor activity under 12/12 light/dark (LD) and dark/dark (DD) cycles. Wheel-running activities in WT (A) and $mPer2^{-/-}$ (B) mice are doubly plotted by aligning two consecutive days horizontally. Five-minute intervals are used to indicate the accumulation of wheel revolutions. Mice were entrained in the LD condition for two weeks, and then subjected to the DD condition for 10 days. Gray area indicates the DD period.

Bone Marrow and RNA Extraction

Mice were sacrificed by cervical dislocation at ZT/CT 0, 4, 8, 12, 16, and 20 (n = 4–5/per timepoint) (ZT 0 = lights-on at 06:00 h; ZT 12 = lights-off at 18:00; CT 12 = onset of active phase.) Both sides of the femur of each mouse were removed, and the bone marrow flushed with PBS using a syringe. All bone marrows for each timepoint (n = 4–5) were mixed together, and whole bone marrow was collected by a quick centrifugation. Total RNA was purified according to the instructions provided by the manufacturer of the Trizol Reagent (TianGen, Beijing, China). RNA quality was determined by ND3000 and a 1% nondenaturing agarose gel.

Reverse Transcription and Q-RT-PCR

To generate single-strand cDNA, 2 μg total RNA was used as the starting template for first strand cDNA synthesis using M-MLV Protoscript kit (NEB) according to the user's manual. RT-PCR for mouse *Dap-10*, *Ly49C*, *Ly49I*, *Rac1*, *Mapk1*, *Map2k1*, *Nkg2d*, *Shp-1*, *Pak1*, *Pik3ca*, *Vav1*, *Per1*, *Bmal1*, *Clock*, and *Rev-erbα* was carried out. Primers for real-time PCR were designed using ABI primer express software 2.0, as shown in Table 1. The housekeeping gene *18s* was used as an internal control because of its constant expression during the day. An optimal amount of cDNA was mixed with real-time primer and SYBRI (TianGen, Beijing, China) master mixture to a final volume of 20 μl according to the protocol, and real-time PCR was carried out in a BIO-RAD DNA Engine OPTICON 2. Each sample was analyzed in triplicate to ensure the

TABLE 1 Primer sequence for real time quantitative RT-PCR

Gene	Genebank ID	Primers	Sequence
Dap-10	NM_011827	F	5′AGTTTTGGCCAGATCCCTTCA
		R	5′TGCCGATGTCTGACTTGCAG
Ly49C	NM_010648	F	5′CATGGAGTGGATGTAAAGCGAA
		R	5′GGCGTTGAAGGAATTTCAGTTC
Ly49I	NM_010651	F	5′GAGAACAGGACAGATGGAACAGTG
		R	5′AACCAGTGTTTAACACCTCTGCCT
Racl	NM_009007	F	5′ATCCCCACCGTCTTTGACAAC
		R	5′TGTCCAGCTGTGTCCCATAGG
Mapkl	NM_011949	F	5′CCTGGAGCAGTATTATGACCCAAG
		R	5′GGTAAGTCGTCCAACTCCATGTC
Map2kl	NM_008927	F	5′GTGCAACTCCCCGTACATCG
		R	5′AAGGACCCACCATCCATGTG
Nkg2d	NM_001083322	F	5′CCTGTTTGTCTCAAAATTCCAGCC
		R	5′TCCCATCCAGTGATAGGACTTAACC
Shp-1	NM_001077705	F	5′GCTTATGGAAAGCATCTCCACC
		R	5′AAGGACCCACCATCCATGTG
		R	5′CGCTGTGCTCGTACCATCTG
Pakl	NM_011035	F	5′TCTGAGACCCCAGCAGTACCA
		R	5′GCGTGGAGCAATCACTGGA
PikSca	NM_008839	F	5′CTGCATCAATGGCTCAAGGAC
		R	5′CAAGATAAAGGTTGCCACGCA
Vavl	NM_011691	F	5′AGTGCATCCCTATGTCCACGG
		R	5′TCCCATCAGAACGGTTGGTG
Perl	NM_011065	F	5′CGGATTGTCT ATATTTCGGAGCA
		R	5′GGGC ACCCCGAAAC ACA
Bmall	NM_007489	F	5′TCGTTGCAATCGGGCG
		R	5′CCGT ATTTCCCCGTTCGC
Clock	NM_007715	F	5′-CTTTCCTTCCTT AGAGACGAGACTG
		R	5′-GGTCTTGGTGCTCATGTGC A
Rev-erb a	NM_145434	F	5′GGATGCCCGTCTGCCC
		R	5′TCAGCGCTTC ATT ATGACGC
18s	NR_003278	F	5′CTTTGGTCGCTCGCTCCTC
		R	5′CTC ACCGGGTTGGTTTTG AT

F = Forward Primer; R = Reverse Primer

accuracy of the data. PCR conditions were as follows: 10 min at 95°C 40 cycles of 94°C for 20 sec, 60°C for 20 sec, and 72°C for 20 sec. At the end of each extension step, fluorescence was measured at 79°C to eliminate the background fluorescence from primer dimers. Melting curves were done when the cycles finished, every 1° from 70° to 95°C to adjust for product specificity. The relative quantity of each gene over the time series was determined by first normalizing to the 18S housekeeping gene profile, then calibrated to its own nadir over the time series, based on the arithmetic formula $2^{-\Delta\Delta Ct}$, as described in the manual. Briefly, relative mRNA expression intensity (REI) was calculated as

$$\{\text{REI } A_i = \text{Power}(2, \text{Max}\Delta(\text{CtA} - \text{Ct18s}) - \Delta(\text{CtA}_i - \text{Ct18s}_i))\}$$

where *REI* A_i indicates the calculation of relative mRNA expression intensity of *A* gene at i time point. CtA_i represents the Ct value of A gene in *i* timepoint from RT-PCR, and $Ct18s_i$ stands for the Ct value of *18s* in the same time point. $\triangle(CtA_i\text{-}Ct18s_i)$ is the difference Ct value between gene *A* and *18s* at i timepoints. $Max\triangle(CtA\text{-}Ct18s)$ represents the maximum difference Ct value between gene *A* and *18s* throughout all the investigated timepoints. Thus, REI in this study represents the fold changes of gene expression level for each gene, compared to its lowest expression value 1 (power (2, 0) throughout the whole investigated time.

FACS Analysis of NK, NKT, and T Cells Population in Bone Marrow

1.5×10^6 bone marrow cells pooled from three mice were labeled with PE Hamster Anti-mouse CD49b (Cat: 558759, BD Pharmingen™) and PerCP Anti-mouse CD3ϵ (Cat: 100325, Biolegend) antibodies at room temperature for 20 min, protected from light. Labeled cells were applied to flow cytometric analysis immediately after PBS washing with Coulter Epics XL (Beckman), and 100,000 events were acquired.

Cyclic Gene Expression Analysis and Statistical Analysis

Time effects for gene expression in WT and $mPer2^{-/-}$ mice (LD and DD) were analyzed by one-way analysis of variance (ANOVA). Then, cosine regression analysis (CRA) of cyclic gene expression was performed using SPSS 13.0 statistics software. Here, we used the methods described by Peter Watson, MRC Cognition & Brain Sciences Unit and others (Nelson et al., 1979; Stolwijk et al., 1999). The cosine model for cyclic gene expression analysis is as follows:

$$\{\mathrm{f(t)} = \mathrm{M} + \mathrm{Amp} \times \mathrm{Cos}(2\pi\mathrm{t}/\mathrm{T} + \phi) + \varepsilon_\mathrm{t}\}$$

where *f(t)* = relative gene expression intensity; *M* = intercept (mesor); *Amp* = amplitude; ϕ = acrophase (peak time); *T* = trial period (in h) in the present study 24 or 12 h; ε_t = residual error. This cosine regression function is equivalent to the following linear regression function:

$$\{\mathrm{f(t)} = \mathrm{M} + \mathrm{A} \times \mathrm{Cos}(2\pi\mathrm{t}/\mathrm{T}) + \mathrm{B} \times \mathrm{Sin}(2\pi\mathrm{t}/\mathrm{T})\}$$

where M = intercept (mesor); *A* and *B* are predictors for this function; and *T* = trial period (in h) in the present study 24 or 12 h. *AMP* and ϕ were calculated from the predicted value of *A* and *B*, where $Amp = square(A^2+B^2)$ and $\phi = ArcTan(-B/A)$. Based on this regression model, linear regression was carried out for analyzing cyclic gene expression in WT and $mPer2^{-/-}$ mice under both LD and DD conditions. Summary of

cyclic gene expression was done only when the p value from ANOVA and CRA and the p value for M, A, and B prediction < 0.05.

Figures were drawn with Origin software and processed with Adobe Illustrator CS3. Data are expressed as mean ± SEM. Comparisons of gene expression between WT and *mPer2*$^{-/-}$ mice were performed with one-way ANOVA with the Tukey LSD post-test or two-way ANOVA with Bonferroni post-test. A value of $p < 0.05$ was considered statistically significant.

RESULTS

Level of mRNA Expression of Ly49C, Ly49I, and Nkg2d Was Significantly Downregulated in mPer2$^{-/-}$ Mice Bone Marrow

In order to investigate how genes participating in the cytotoxic process and IFN-γ production pathway were affected by loss of *mPer2* functions, expressions of 11 key genes (viz., *Dap-10, Ly49C, Ly49I, Rac1, Mapk1, Map2k1, Nkg2d, Shp-1, Pak1, Pik3ca*, and *Vav1)* were measured by Q-RT-PCR. Considering that expression of these genes may vary throughout the day, bone marrows were collected from mice every 4 h (n = 4) during the day and pooled together. Overall mean mRNA expression of each gene was compared between WT and *mPer2*$^{-/-}$ mice. As shown in Figure 2, most of the genes did not show significant differences in their mRNA expression level in WT mice, compared with

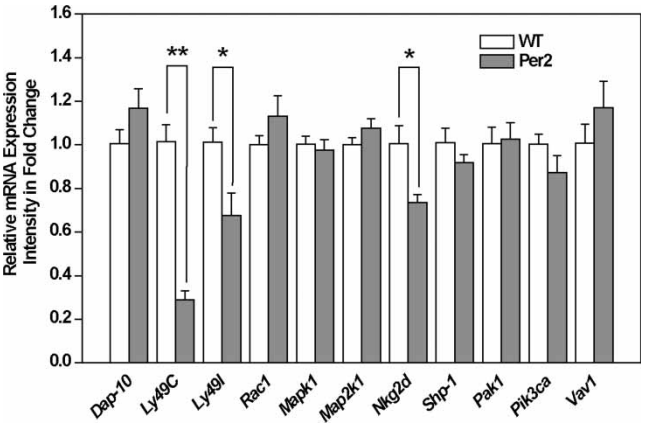

FIGURE 2 Overall mRNA expression comparison of cytotoxicity regulation genes in bone marrow between wild-type (WT) (white bar) and *mPer2*$^{-/-}$ (gray bar) mice. Bone marrow of mice entrained under LD conditions were collected throughout the day at 4 h intervals (n = 4 animals/timepoint) and pooled together. Real-time quantitative RT-PCR was carried out with each gene individually in triplicate. Relative mRNA expression was calculated in fold change. The amount of mRNA expression in *Ly49C*, *Ly49I*, and *Nkg2d* was downregulated in *mPer2*$^{-/-}$ mice. *significant difference of gene expression between WT and *mPer2*$^{-/-}$ mice with a p value < 0.05 from one-way ANOVA. **$p < 0.001$.

mPer2$^{-/-}$ mice. Unexpectedly, mRNA expressions of *Ly49C* ($p < 0.001$), *Ly49I* ($p = 0.039$), and *Nkg2d* ($p = 0.038$) were significantly downregulated in *mPer2*$^{-/-}$ mice bone marrow (see Figure 2). These three genes encode three key transmembrane receptors that mediate the activation (*Nkg2d*) or inhibition (*Ly49C* and *Ly49I*) of cytotoxicity processes and IFN-γ production.

Loss of mPer2 Function Abolished Daily Circadian Oscillations of Ly49C, Ly49I, Nkg2d, Per1, and Rev-erbα in the Bone Marrow of WT Mice Maintained under LD

Because expressions of *Ly49C, Ly49I*, and *Nkg2d* were significantly downregulated in *mPer2*$^{-/-}$ mice, rhythmic expression of these genes was of interest. We selected three of the cytotoxic genes (*Ly49C, Ly49I*, and *Nkg2d*) that exhibited highly different expression between WT and *mPer2*$^{-/-}$ mice to adjust their cyclic expression in bone marrow under LD, as well as three others (*Mapk1*, *Shp-1*, and *Pik3ca*) that did not show significant difference. In addition, the circadian fluctuation of four core clock genes (*Per1*, *Bmal1*, *Clock*, and *Rev-erbα*) were measured. Gene expressions were performed using Q-RT-PCR on total RNA from bone marrow sampled at ZT 0, 4, 6, 12, 16, and 20 (n = 4–5/timepoint). To evaluate the rhythmic features of each gene, one-way ANOVA and single circadian (24 h) or circasemidian (12 h) regression analysis were used to test the significance of a time-effect and cyclic expression (see Table 2). Significant circadian expression rhythmicity was observed for *Per1*, *Rev-erbα*, *Ly49C*, and *Nkg2d* in WT mice bone marrow (see Figure 3). A significant circasemidian fluctuation was found for *Bmal1* and *Pik3ca*. However, in *mPer2*$^{-/-}$ mice, the circadian rhythmic expressions of *Per1*, *Rev-erbα*, and *Nkg2d* were disrupted. Unexpectedly, a dampened circadian rhythm still persisted in *Ly49C* in *mPer2*$^{-/-}$ mice (Amp (WT) = 1.12; Amp (Per2) = 0.59). Consistently, *Mapk1*, *Shp-1*, and *Pik3ca* did not show any significant cyclic mRNA expression rhythms in WT or *mPer2*$^{-/-}$ mice, except for a weak circasemidian fluctuation of *Pik3ca* in WT mice (Amp = 0.21).

A phase chart was plotted with the best fitting model from circadian (24 h) or circasemidian (12 h) regression for the visual comparison of gene expression between WT and *mPer2*$^{-/-}$ mice. As shown in Figure 4, the significant circadian expressed genes of *Rev-erbα* and *Nkg2d* peaked after noon in WT mice. However, *Per1* and *Ly49C* peaked right after the transition from the light to dark phase. In *mPer2*$^{-/-}$ mice (see Figure 4), although most of the cyclic expressions were disrupted, the best-fitting regression showed a higher tendency of peak times for all these investigated genes during the dark phase (active phase).

TABLE 2 Circadian (24 h) and Circasemidian (12 h) analysis for gene expression in bone marrow of zeitgeber time (ZT)

	Time-Effect analysis by ANOVA[a] and Cosine Regression Analysis[b]												
			ANOVA			Cosine Regression Analysis						95% CI for peak[j]	
Gene	G[g]	C[c]	F	*p*	T[d]	F	*p*[e]	M^h	Amp^1	$f(h)^{\#}$	*2Amp%*[f]	L(h)	U[(h)]
*Perl**	WT	LD	155.44	0.000	24	15.20	0.000	1.85	1.07	12.42	116.15	10.95	13.90
$Perl^{NS}$	WT	LD	155.44	0.000	12	2.84	0.090	1.85	0.69	12.32	74.28	10.61	14.03
$Perl^{NS}$	Per2	LD	2.29	0.111	24	6.61	0.009	1.31	0.23	13.79	34.77	11.55	16.03
$Perl^{NS}$	Per2	LD	2.29	0.111	12	0.04	0.961	1.31	0.02	9.77	3.69	-4.66	24.20
$Bmall^{NS}$	WT	LD	10.08	0.001	24	2.64	0.104	1.81	0.19	14.83	21.55	11.29	18.38
*Bmall**	WT	LD	10.08	0.001	12	8.63	0.003	1.81	0.28	13.74	30.88	12.76	14.72
$Bmall^{NS}$	Per2	LD	6.53	0.004	24	2.68	0.101	1.81	0.42	14.89	46.70	11.37	18.41
$Bmall^{NS}$	Per2	LD	6.53	0.004	12	0.33	0.724	1.81	0.17	2.91	18.68	-2.10	7.93
$Clock^{NS}$	WT	LD	8.23	0.001	24	1.85	0.192	1.67	0.25	8.31	29.72	4.07	12.55
$Clock^{NS}$	WT	LD	8.23	0.001	12	1.17	0.338	1.67	0.20	3.76	24.55	1.09	6.42
$Clock^{NS}$	Per2	LD	2.52	0.088	24	1.35	0.290	1.82	0.24	18.95	26.48	13.99	23.92
$Clock^{NS}$	Per2	LD	2.52	0.088	12	2.90	0.086	1.82	0.33	7.21	35.85	5.52	8.90
*Rev-erbα**	WT	LD	22.44	0.000	24	41.93	0.000	2.64	1.40	8.51	106.39	7.62	9.39
$Rev\text{-}erb\alpha^{NS}$	WT	LD	22.44	0.000	12	0.34	0.718	2.64	0.32	7.52	23.97	2.56	12.48
$Rev\text{-}erb\alpha^{NS}$	Per2	LD	0.61	0.697	24	1.08	0.365	2.24	0.28	4.32	25.45	-1.22	9.87
$Rev\text{-}erba\alpha^{NS}$	Per2	LD	0.61	0.697	12	0.56	0.581	2.24	0.21	0.40	18.96	-3.44	4.25
*Ly49C**	WT	LD	17.05	0.000	24	6.21	0.011	6.50	1.12	12.06	34.52	9.75	14.37
*Ly49C**	WT	LD	17.05	0.000	12	5.12	0.020	6.50	1.06	0.91	32.64	-0.37	2.18
*Ly49C**	Per2	LD	7.74	0.002	24	4.73	0.025	1.87	0.59	13.61	63.21	10.97	16.26
$Ly49C^{NS}$	Per2	LD	7.74	0.002	12	0.56	0.580	1.87	0.25	6.54	26.87	2.70	10.38
$Ly491^{NS}$	WT	LD	2.36	0.104	24	3.82	0.046	3.00	0.52	12.02	35.02	9.07	14.96
$Ly49I^{NS}$	WT	LD	2.36	0.104	12	1.36	0.286	3.00	0.35	2.41	23.62	-0.06	4.88
$Ly49I^{NS}$	Per2	LD	3.83	0.026	24	2.25	0.140	2.04	0.64	15.52	63.08	11.68	19.36
*Ly49I**	Per2	LD	3.83	0.026	12	4.14	0.037	2.04	0.80	6.43	78.28	5.01	7.85
$Mapkl^{NS}$	WT	LD	1.90	0.168	24	3.82	0.046	1.49	0.15	15.01	20.61	12.07	17.96
$Mapkl^{NS}$	WT	LD	1.90	0.168	12	0.85	0.448	1.49	0.08	2.42	11.30	-0.71	5.55
$Mapkl^{NS}$	Per2	LD	2.62	0.080	24	2.18	0.147	1.45	0.15	20.14	20.65	16.24	24.04

Continued

TABLE 2 *Continued*

	Time-Effect analysis by ANOVA[a] and Cosine Regression Analysis[b]												
			ANOVA			Cosine Regression Analysis						95% CI for peak[j]	
Gene	G[g]	C[c]	F	*p*	T[d]	F	*p*[e]	*M*[h]	*Amp*[l]	*f(h)*[#]	*2Amp%*[f]	L(h)	U[(h)]
Mapkl^{NS}	Per2	LD	2.62	0.080	12	0.50	0.618	1.45	0.08	9.71	10.85	5.63	13.79
*Nkg2d**	WT	LD	14.46	0.000	24	7.99	0.004	2.82	0.50	8.72	35.18	6.68	10.76
Nkg2d^{NS}	WT	LD	14.46	0.000	12	3.24	0.068	2.82	0.38	1.29	26.88	-0.32	2.89
Nkg2d^{NS}	Per2	LD	7.84	0.002	24	3.26	0.067	1.78	0.30	13.03	33.29	9.84	16.23
Nkg2d^{NS}	Per2	LD	7.84	0.002	12	2.25	0.140	1.78	0.26	8.24	29.05	6.31	10.16
Shp-1^{NS}	WT	LD	1.37	0.303	24	0.17	0.843	1.47	0.08	15.24	11.01	1.39	29.09
Shp-1^{NS}	WT	LD	1.37	0.303	12	3.73	0.048	1.47	0.31	12.87	42.24	11.38	14.36
Shp-1^{NS}	Per2	LD	1.20	0.367	24	2.02	0.168	1.32	0.14	17.32	20.51	13.26	21.38
Shp-1^{NS}	Per2	LD	1.20	0.367	12	1.02	0.384	1.32	0.10	9.21	15.42	6.36	12.05
Pik3ca^{NS}	WT	LD	6.58	0.004	24	2.66	0.102	1.62	0.17	17.53	21.02	14.00	21.06
*PikSca**	WT	LD	6.58	0.004	12	4.62	0.027	1.62	0.21	3.36	25.37	2.03	4.70
Pik3ca^{NS}	Per2	LD	1.88	0.171	24	3.39	0.061	1.55	0.29	18.44	37.89	15.31	21.57
PikSca^{NS}	Per2	LD	1.88	0.171	12	0.50	0.615	1.55	0.13	7.03	17.01	2.96	11.10

[a] Analysis of Variance for gene expression difference among the experiment time points. [b] Analysis of Circadian (24 h) or Circasemidian (12 h) rhythm for gene expression using Cosine Regression Analysis (CRA) (refer to methods for details). [c] Lighting condictions, LD = 12 h/12 h light/dark, DD = 12 h/12 h dark/dark. [d] Period for CRA model. [e] *p* value for CRA. [f] double amplitude = range from trough to peak of CRA model as % of mesor. [s] genotype of experiment mice, WT = C57 BL/6 WT mice. Per2 = *mPer2* knockout mice. [h] Mesor of CRA model.[l] Half range from trough to peak of CRA model. [#] Time (hours) of peak from CRA model.[j] 95% Confidence Interval for peak (in hours). * Significance in circadian or circasemidian CRA model only when *p* value from ANOVA, CRA and *p* value for M, A, B prediction (descibed in methods) all < 0.05. [NS]None significance in circadian or circasemidian CRA model.

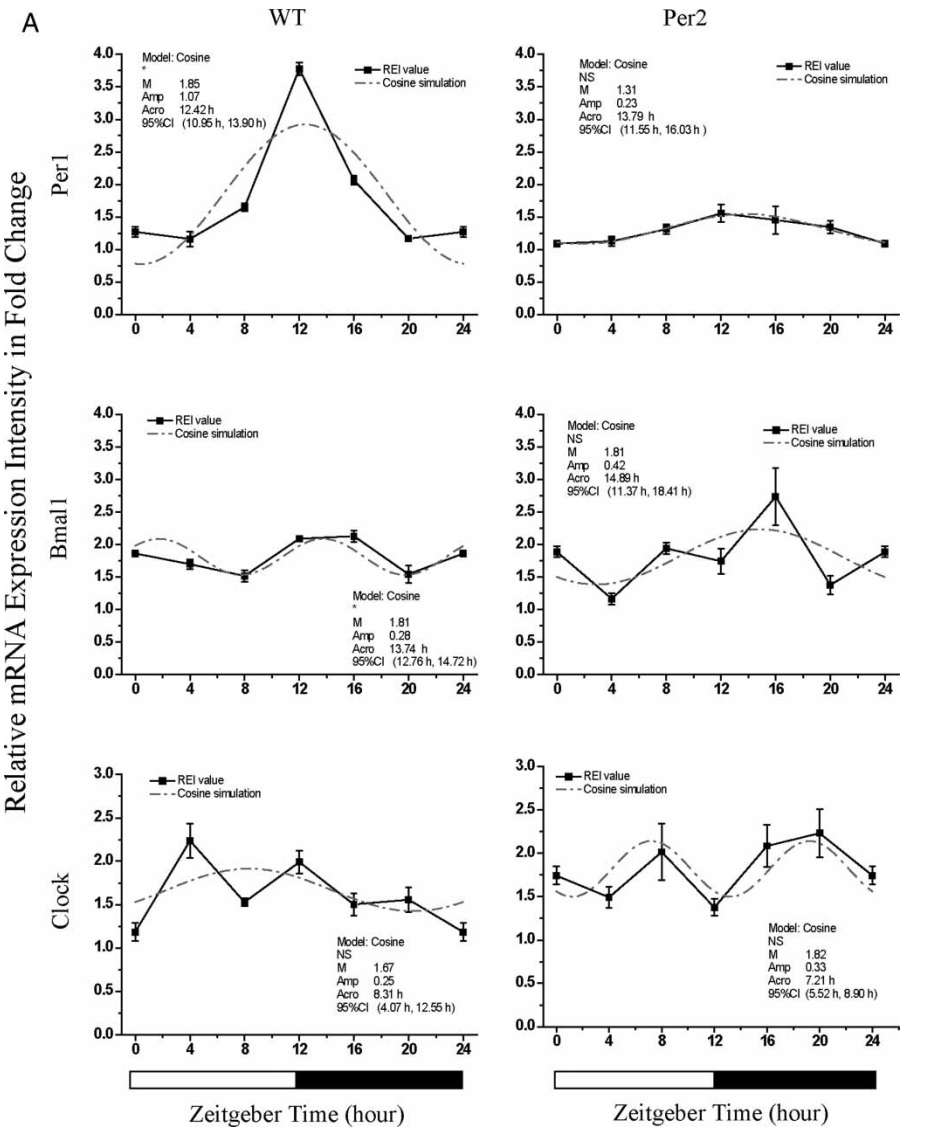

FIGURE 3 Cyclic gene expression profiling for *Per1*, *Bmal1*, *Clock*, *Rev-erbα*, *Ly49CLy49I*, *Mapk1*, *Nkg2d*, *Shp-1*, and *Pik3ca* in the bone marrow of WT and $mPer2^{-/-}$ mice entrained under LD cycles. Real-time quantitative RT-PCR was used to measure the gene expression. Relative mRNA expression intensity at each timepoint was calculated as fold change. Each value represents the mean ± SEM (n = 3, triplicate in RT-PCR repeat). ZT0 was doubly blotted as ZT24 in this figure. Relative mRNA expression intensity (REI) value is drawn as a solid black line. The cosine simulation from the best-fitting circadian (24 h) or circasemidian (12 h) cosine model regression analysis (CRA) is drawn in dash-dot line. The values of mesor (M), amplitude (Amp), acrophase (acro, ϕ), and 95% CI for acrophase from CRA are attached as well. White bars at the bottom of the figure represent light phase (lux = 185 ± 5) and black bars represent the dark phase (lux = 0.05 ± 0.01). Time-effect was analyzed with one-way ANOVA and cosine regression analysis. *summary at cyclic gene expression only when p value from ANOVA and CRA and p value for M, Amp, and ϕ prediction < 0.05. Abbreviation: NS = not significant.

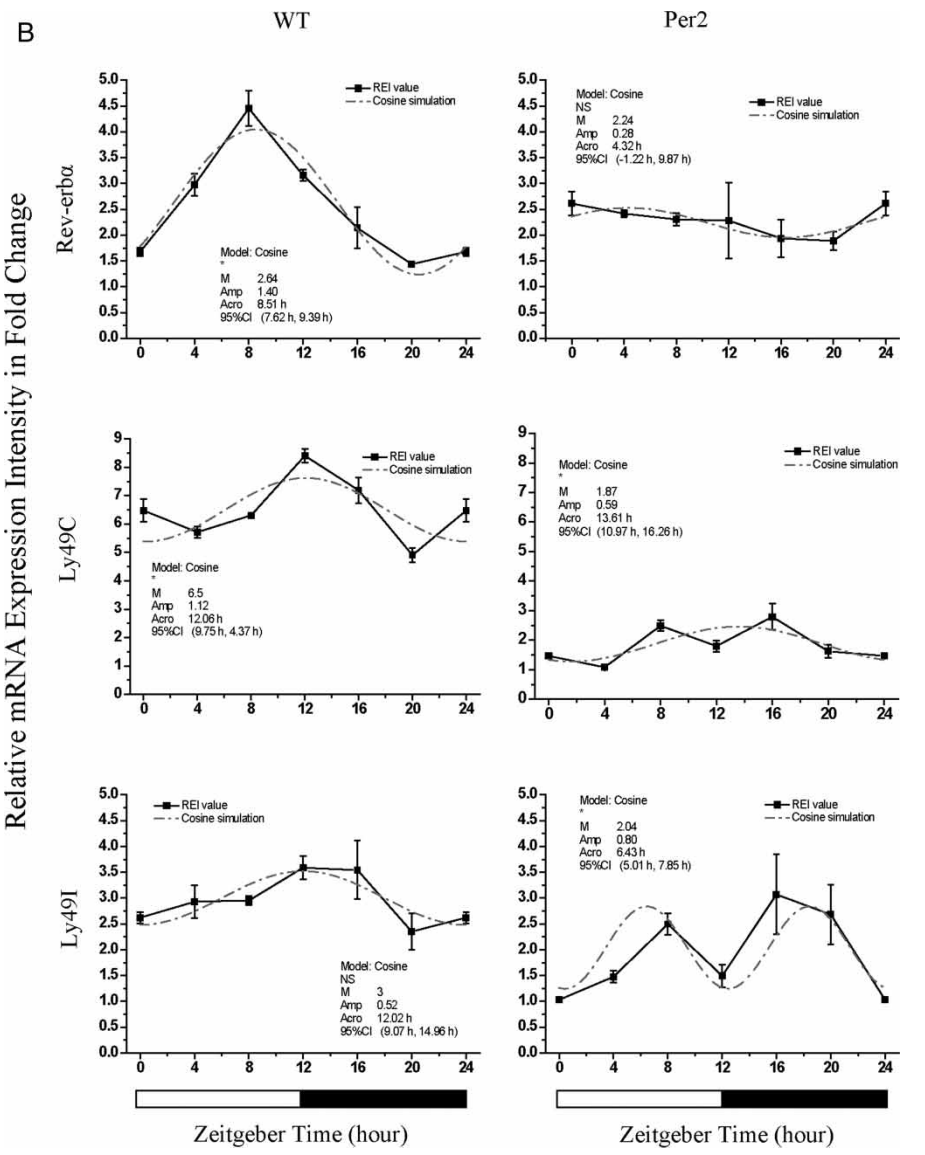

FIGURE 3 Continued

A best-fitting mesor plot was also constructed to compare the overall gene expression between WT and *mPer2*$^{-/-}$ mice. As shown in Figure 5, *mPer2* knockout significantly led to downregulation of overall mRNA expression in *Per1*, *Rev-erbα*, *Ly49C*, *Ly49I*, and *Nkg2D*, which is consistent with the data shown in Figure 2. Taken together, our results suggest the expression of *Ly49C* and *Nkg2D* in bone marrow is under circadian control, where *mPer2* acts as a positive modulator, rather than a negative

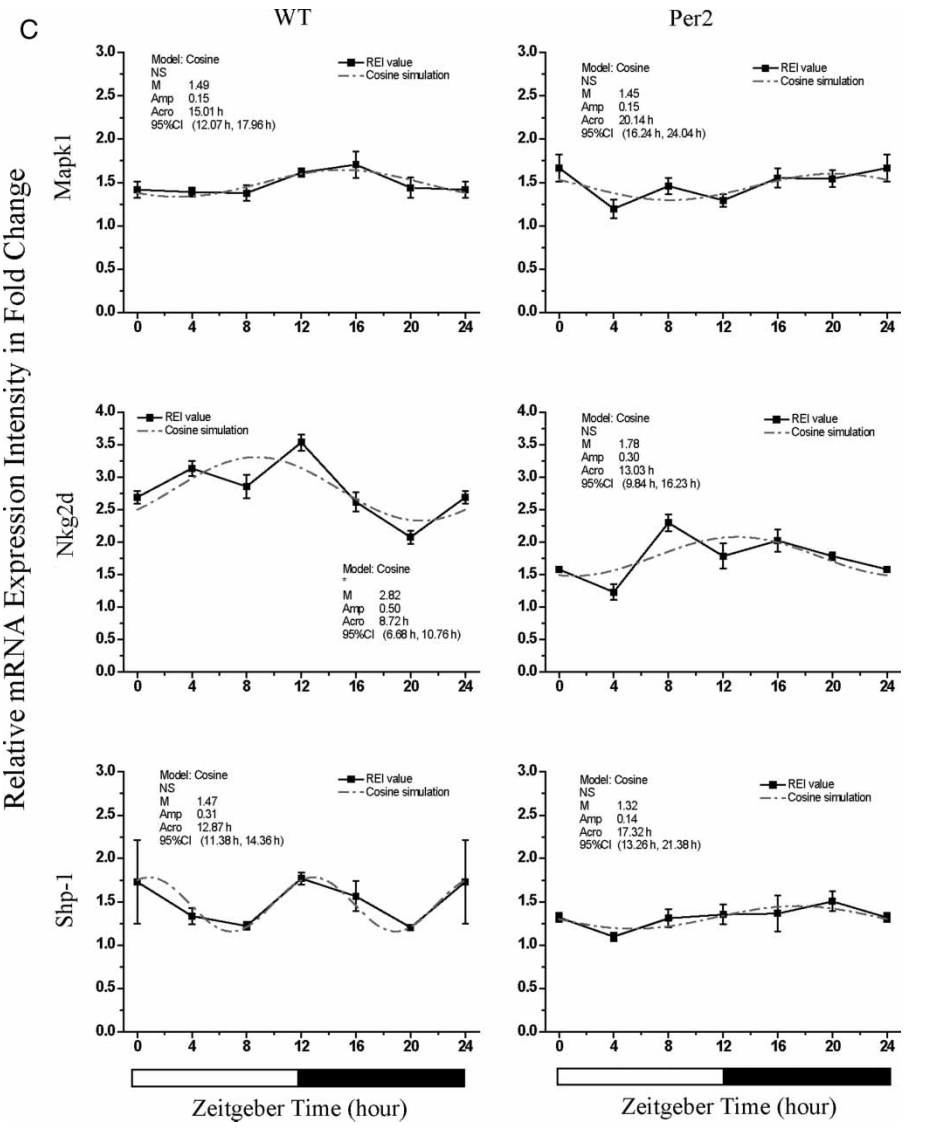

FIGURE 3 Continued

component, as in the positive-negative transcriptional translational feedback loop.

Expression Profiling in Free-Running (DD) Cycles Reconfirm Positive Regulation by mPer2 on Modulating Ly49C and Nkg2d Expression in Bone Marrow

In order to confirm the circadian oscillation and overall expression characteristics of *Ly49C, Nkg2d, Per1*, and *Rev-erbα* in WT and *mPer2*$^{-/-}$

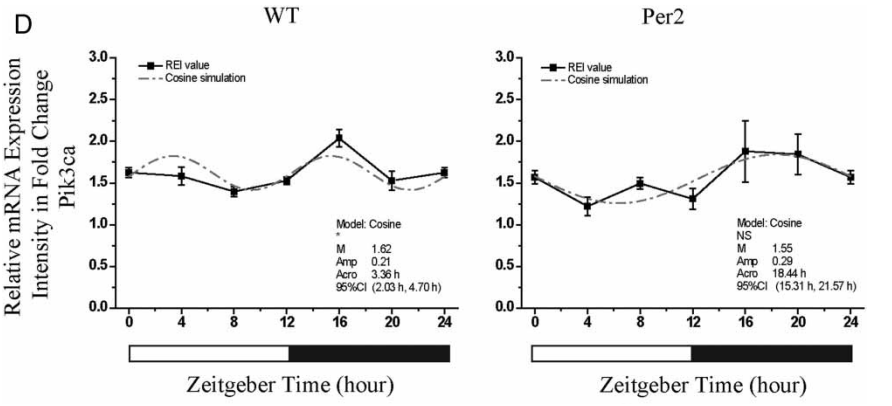

FIGURE 3 Continued

mice under LD cycles, the time-dependence of gene expression profiling was conducted under free-running cycles (DD) every 4 h during the 24 h. Cyclic gene expression was analyzed with one-way ANOVA and single circadian (24 h) or circasemidian (12 h) regression analysis. A detailed list of time-effect parameters is shown in Table 3. As seen in Figure 6, consistent with what we observed in LD cycles, significant circadian expression rhythmicity was observed for *Per1*, *Rev-erbα*, *Ly49C*, and *Nkg2d* in WT mice bone marrow under DD cycles. Unexpectedly, significant circadian expression was observed for *Bmal1*, *Clock*, *Ly49I*, *Mapk1*, *Shp-1*, and *Pik3ca* in DD, while no significant circadian rhythms could be found in LD cycles. The phase plot in Figure 4C shows that all of the investigated genes, except *Per1* and *Rev-erbα*, reached their acrophase at a similar time—the middle of the subjective day (rest phase). *Per1* and *Rev-erbα* achieved their acrophase similarly with that in LD cycles (see Figures 4A and 4C).

Expression profiling in $mPer2^{-/-}$ mice showed that significant, but dampened, circadian rhythms still persisted for *Per1* (Amp (WT) = 1.03; Amp (Per2) = 0.33), *Rev-erbα* (Amp (WT) = 23.73; Amp (Per2) = 4.75), *Ly49C* (Amp (WT) = 3.35; Amp (Per2) = 1.56), *Nkg2d* (Amp (WT) = 4.32; Amp (Per2) = 1.53), and *Pik3ca* (Amp (WT) = 1.76; Amp (Per2) = 0.70), as shown in Figure 4. A significant co-phase of circasemidian (12 h) rhythmicity was found for *Bmal1* and *Ly49I*. The circadian rhythms of *Clock*, *Mapk1*, and *Shp-1* were disrupted. The acrophase plot in Figure 4D shows that most of these genes reached their acrophase still in the subjective day (rest phase). Overall expression based on the mesor values in Figure 5B consistently showed that the expression of *Rev-erbα*, *Ly49C*, and *Nkg2d* was significantly downregulated in $mPer2^{-/-}$ mice. In contrast, expression of *Bmal1* was upregulated in DD instead of

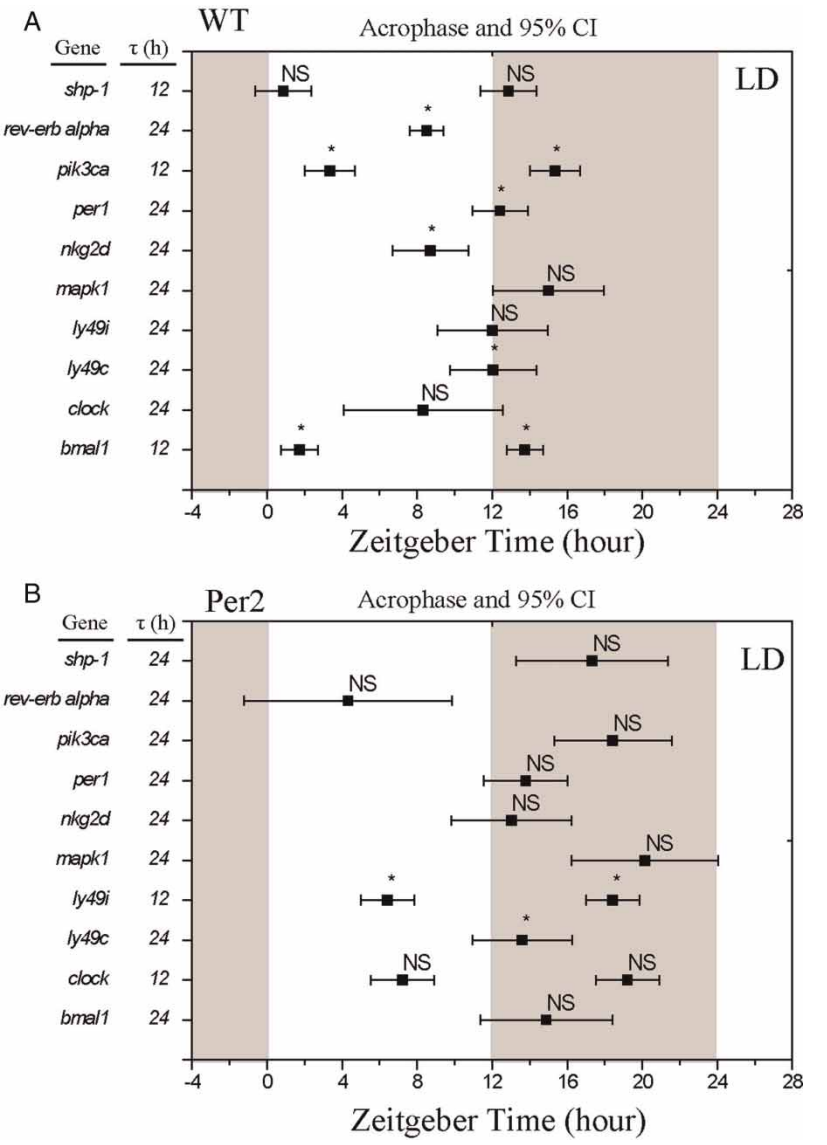

FIGURE 4 Comparison of acrophase between WT and *mPer2*$^{-/-}$ mice under LD and DD cycles. Acrophase and 95% confidence interval (CI) from the best-fitting cosine regression model is plotted across zeitgeber time for WT (A), *mPer2*$^{-/-}$ mice (B), circadian time for WT (C), and *mPer2*$^{-/-}$ mice (D). τ = period in h. Gray areas in (A) and (B) denote the dark period (active phase). Gray areas in (C) and (D) denote dark period, while dark gray areas indicate the subject night (active phase). NS = not significant in cyclic gene expression regression. *significant circadian or circasemidian gene expression regression.

downregulated in LD cycles. Taken together, expression profiling reconfirmed that *mPer2* positively modulates the circadian expression of *Ly49C* and *Nkg2d*.

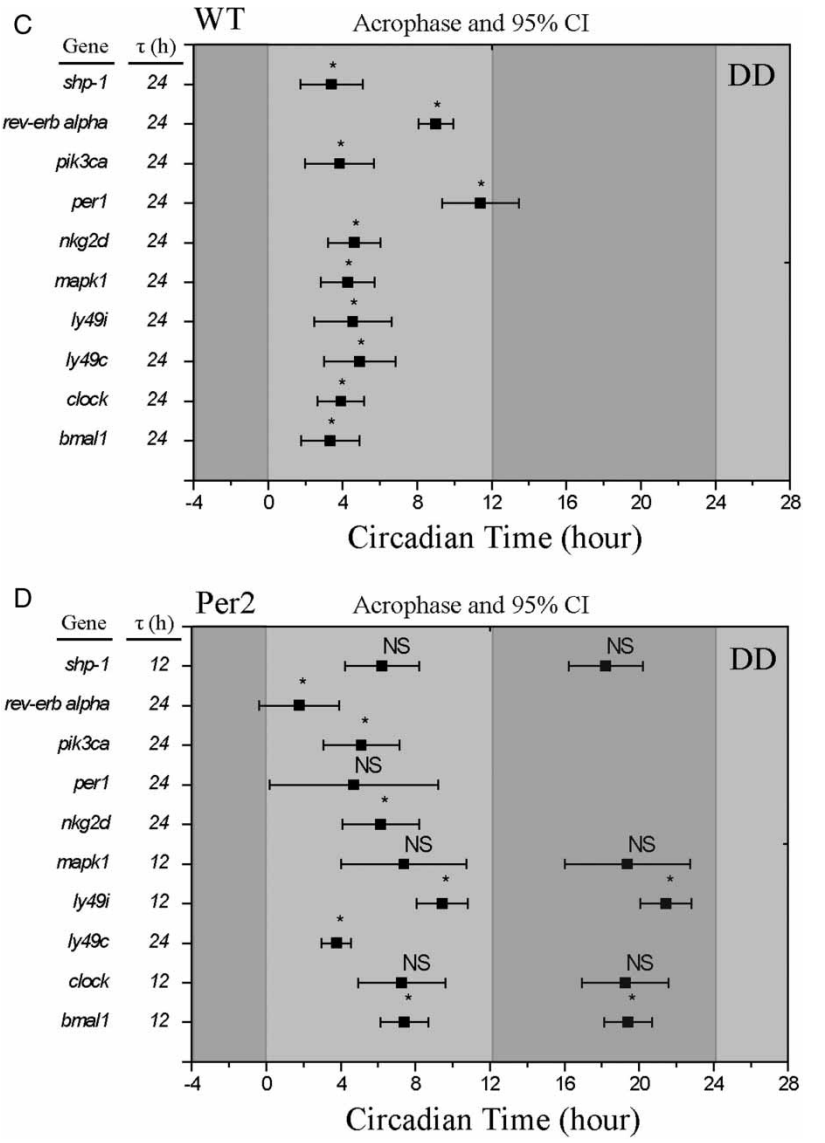

FIGURE 4 Continued

Insignificant Daily Variation of NK, NKT, and T Cells Population in Bone Marrow

The cyclic expression of these genes in bone marrow could be due to either the endogenous molecular circadian clock regulation or fluctuation of the cell population from which these genes were expressed. To discern between these possibilities, the daily oscillation of cell numbers of NK,

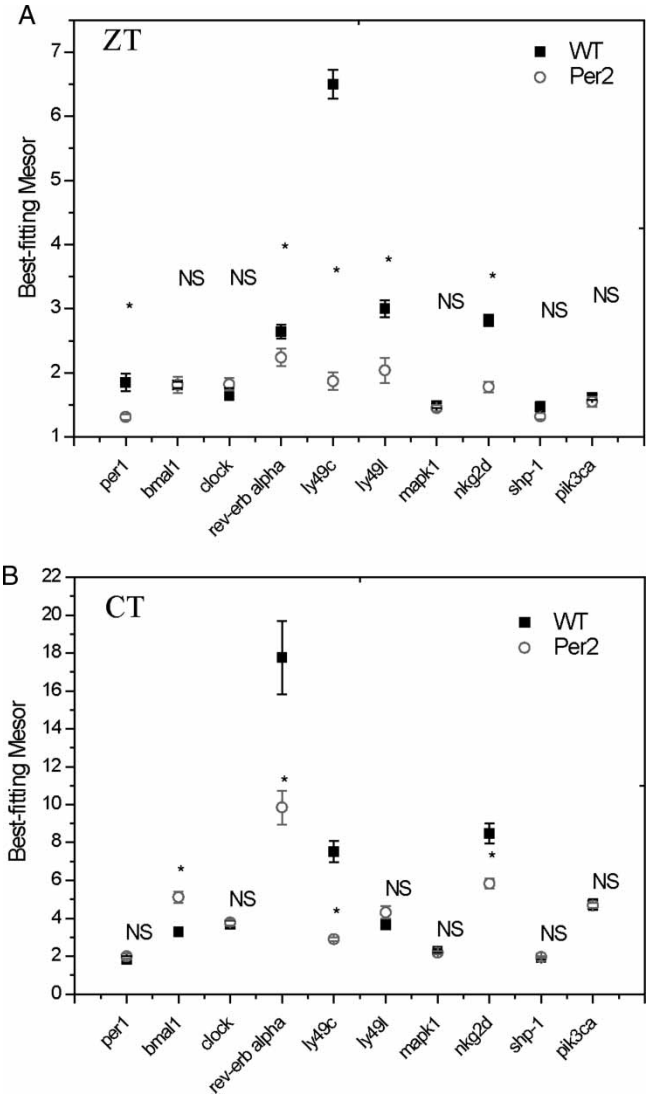

FIGURE 5 Comparison of mesor between WT and $mPer2^{-/-}$ Mice in ZT (A) and CT (B) cycles. Best-fitting mesor from cosine regression analysis for each gene is shown. Mesor of WT mice is drawn with filled square. Mesor of $mPer2^{-/-}$ mice is drawn with open circle. *significant difference of mesor between WT and $mPer2^{-/-}$ mice with a p value < 0.05 from one-way ANOVA. Abbreviation: NS = non-significance between WT and $mPer2^{-/-}$ mice with a p value > 0.05 from one-way ANOVA.

NKT, and T cells in bone marrow were analyzed by FACS. As shown in Figures 7 and 8, there was no significant difference in the numbers of NK ($p = 0.132$), NKT ($p = 1$), and T cells ($p = 0.221$) in bone marrow, suggesting the cyclic expression of these genes are controlled by endogenous molecular clocks.

TABLE 3 Circadian (24 h) and Circasemidian (12 h) analysis for gene expression in bone marrow of circadian time (CT)

	Time-Effect analysis by ANOVA[a] and Cosine Regression Analysis[b]												
			ANOVA			Cosine Regression Analysis						95% CI for peak[j]	
Gene	G[g]	C[c]	F	*p*	T[d]	F	*p*[e]	*M*[h]	*Amp*[i]	*f(h)*[#]	*2Amp%*[f]	L(h)	U(h)
mPerl *	WT	DD	134.77	0.000	24	7.81	0.005	1.84	1.03	11.38	111.42	9.32	13.44
mPerl *	WT	DD	134.77	0.000	12	4.93	0.023	1.85	0.91	11.53	98.18	10.23	12.83
mPerl^{NS}	Per2	DD	6.94	0.003	24	1.63	0.229	1.99	0.33	4.70	32.94	0.18	9.21
mPerl^{NS}	Per2	DD	6.94	0.003	12	1.63	0.230	1.99	0.33	5.79	32.92	3.53	8.05
mBmall *	WT	DD	42.92	0.000	24	13.78	0.000	3.30	1.22	3.34	73.73	1.79	4.89
mBmall^{NS}	WT	DD	42.92	0.000	12	2.24	0.141	3.30	0.73	10.37	43.99	8.45	12.29
mBmall^{NS}	Per2	DD	22.52	0.000	24	2.68	0.101	5.10	1.11	7.52	43.56	4.00	11.04
mBmall *	Per2	DD	22.52	0.000	12	5.01	0.022	5.11	1.37	7.41	53.69	6.13	8.70
mClock *	WT	DD	28.07	0.000	24	21.47	0.000	3.69	1.75	3.90	94.93	2.66	5.14
mClock^{NS}	WT	DD	28.07	0.000	12	1.57	0.241	3.69	0.85	9.29	45.87	6.99	11.58
mClock^{NS}	Per2	DD	1.22	0.357	24	0.92	0.418	3.77	0.30	6.93	16.11	0.94	12.92
mClock^{NS}	Per2	DD	1.22	0.357	12	1.53	0.247	3.77	0.38	7.27	20.03	4.94	9.59
*mRev-erbα**	WT	DD	99.48	0.000	24	37.89	0.000	17.76	23.73	9.01	267.32	8.07	9.94
mRev-erbα^{NS}	WT	DD	99.48	0.000	12	1.13	0.350	17.77	9.38	8.83	105.60	6.12	11.55
*mRev-erbα**	Per2	DD	6.17	0.005	24	7.10	0.007	9.85	4.75	1.76	96.51	−0.40	3.93
mRev-erbα^{NS}	Per2	DD	6.17	0.005	12	0.33	0.725	9.84	1.40	3.11	28.36	−1.91	8.14
*Ly49C**	WT	DD	17.52	0.000	24	9.00	0.003	7.53	3.35	4.92	89.02	3.00	6.85
*Ly49C**	WT	DD	17.52	0.000	12	3.74	0.048	7.53	2.62	9.37	69.55	7.89	10.86
*Ly49C**	Per2	DD	45.77	0.000	24	59.78	0.000	2.90	1.56	3.76	107.88	2.98	4.54
Ly49C^{NS}	Per2	DD	45.77	0.000	12	0.26	0.771	2.96	0.33	8.85	22.18	3.42	14.27
Ly491 *	WT	DD	22.64	0.000	24	7.71	0.005	3.66	1.33	4.54	72.69	2.46	6.61

Ly491 *	WT	DD	22.64	0.000	12	4.94	0.022	3.66	1.18	9.60	64.39	8.31	10.90
Ly491^{NS}	Per2	DD	7.45	0.002	24	0.87	0.437	4.31	0.72	6.63	33.46	0.47	12.79
*Ly49I**	Per2	DD	7.45	0.002	12	4.38	0.032	4.31	1.35	9.44	62.87	8.07	10.82
*Mapkl**	WT	DD	20.26	0.000	24	16.19	0.000	2.28	0.81	4.27	71.33	2.83	5.70
Mapkl^{NS}	WT	DD	20.26	0.000	12	1.95	0.177	2.28	0.45	9.74	39.22	7.68	11.80
Mapkl^{NS}	Per2	DD	0.61	0.693	24	0.48	0.625	2.19	0.11	3.22	10.30	−5.06	11.49
Mapkl^{NS}	Per2	DD	0.61	0.693	12	0.73	0.498	2.19	0.14	7.38	12.45	4.00	10.75
*Nkg2d**	WT	DD	67.45	0.000	24	16.43	0.000	8.47	4.32	4.62	102.02	3.20	6.04
Nkg2d^{NS}	WT	DD	67.45	0.000	12	2.06	0.162	8.48	2.42	9.27	57.17	7.27	11.28
*Nkg2d**	Per2	DD	6.45	0.004	24	7.83	0.005	5.83	1.53	6.14	52.44	4.08	8.20
Nkg2d^{NS}	Per2	DD	6.45	0.004	12	1.33	0.294	5.83	0.83	10.48	28.48	7.98	12.97
*Shp-1**	WT	DD	28.93	0.000	24	11.79	0.001	1.92	0.49	3.41	50.65	1.73	5.09
Shp-l^{NS}	WT	DD	28.93	0.000	12	3.05	0.077	1.92	0.33	9.85	34.86	8.20	11.50
Shp-1^{NS}	Per2	DD	0.78	0.580	24	0.01	0.989	1.95	0.01	19.11	1.37	-35.29	73.51
Shp-l^{NS}	Per2	DD	0.78	0.580	12	2.09	0.158	1.95	0.16	6.21	16.56	4.21	8.20
*Pik3ca**	WT	DD	18.01	0.000	24	9.78	0.002	4.72	1.76	3.83	74.55	1.98	5.67
PikSca^{NS}	WT	DD	18.01	0.000	12	3.42	0.060	4.72	1.31	9.35	55.49	7.79	10.90
*PikSca**	Per2	DD	3.69	0.030	24	8.09	0.004	4.68	0.70	5.10	29.74	3.08	7.13
PikSca^{NS}	Per2	DD	3.69	0.030	12	0.47	0.634	4.68	0.23	4.89	10.04	0.70	9.09

[a] Analysis of Variance for gene expression difference among the experiment time points. [b] Analysis of Circadian (24 h) or Circasemidian (12 h) rhythm for gene expression using Cosine Regression Analysis (CRA) (refer to methods for details). [c] Lighting conditions, LD = 12 h/12 h light/dark, DD = 12 h/12 h dark/dark. [d] Period for CRA model. [e]*p* value for CRA. [f] double amplitude = range from trough to peak of CRA model, as % of mesor. [g] genotype of experiment mice, WT = C57 BL/6 WT mice, Per2 = mPer2 knockout mice. [h] Mesor of CRA model.[I] Half range from trough to peak of CRA model. [#] Time (in hours) of peak from CRA model.[J] 95% Confidence Interval for peak (in hours). * Significance in circadian or circasemidian CRA model only when *p* value from ANOVA, CRA and *p* value for M, A, B prediction (descibed in methods) all < 0.05. [NS]None significance in circadian or circasemidian CRA model.

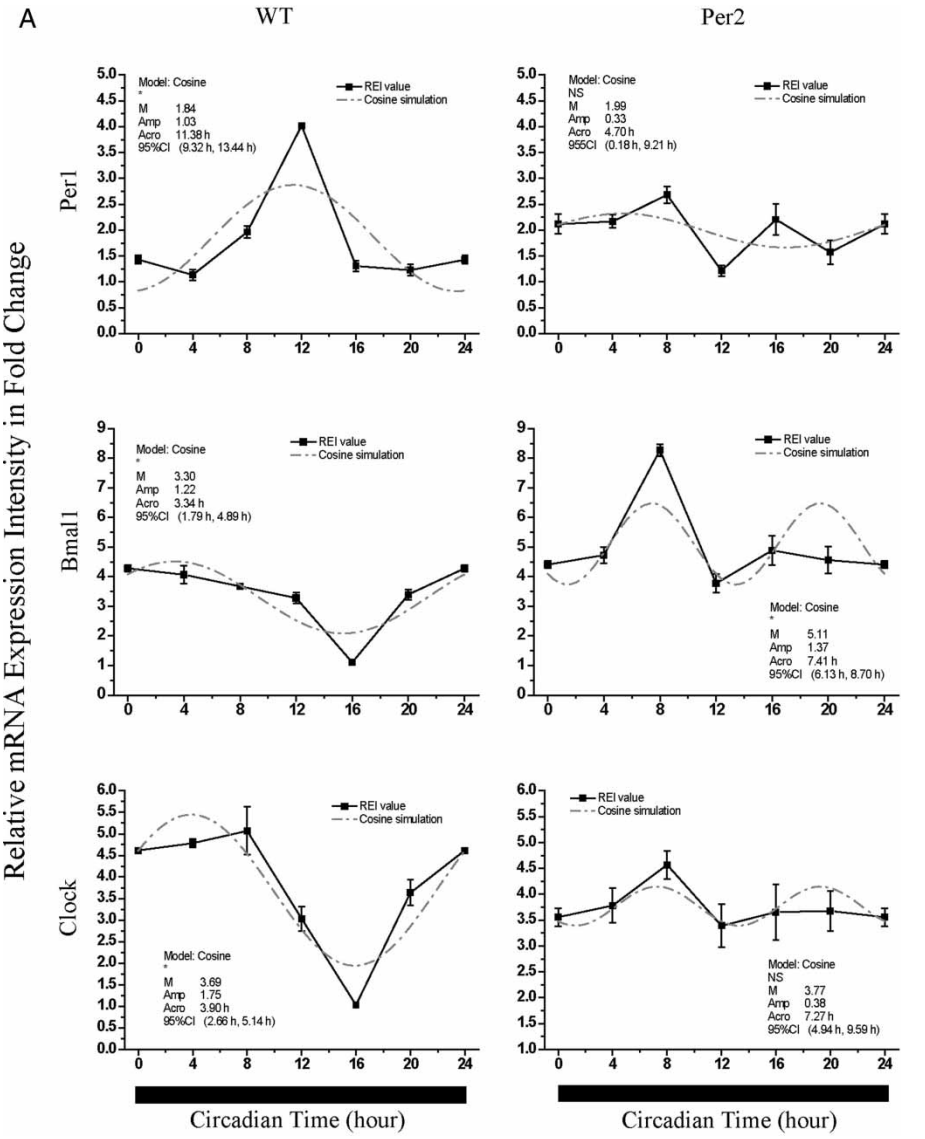

FIGURE 6 Reconfirmation of cyclic gene expression profiling for *Per1*, *Bmal1*, *Clock*, *Rev-erbα*, *Ly49C, Ly49I*, *Mapk1*, *Nkg2d*, *Shp-1*, and *Pik3ca* in the bone marrow of WT and $mPer2^{-/-}$ mice entrained under DD cycles. Calculation of relative mRNA expression is the same as in LD cycles. Same methods for time-effect analysis were applied as well. Relative mRNA expression intensity (REI) value is drawn in solid black line. The cosine simulation from the best-fitting circadian (24 h) or circa-semidian (12 h) cosine model regression analysis (CRA) is drawn in dash-dot gray line. Each value represents the mean ± SEM (n = 3, triplicate in RT-PCR repeat). CT0 was doubly blotted as CT24 in this figure. Determination of each CT timepoint was adjusted by using a running-wheel facility. *summary at cyclic gene expression only when p value from ANOVA and CRA and p value for M, Amp, and ϕ prediction are < 0.05. Abbreviation: NS = not significant.

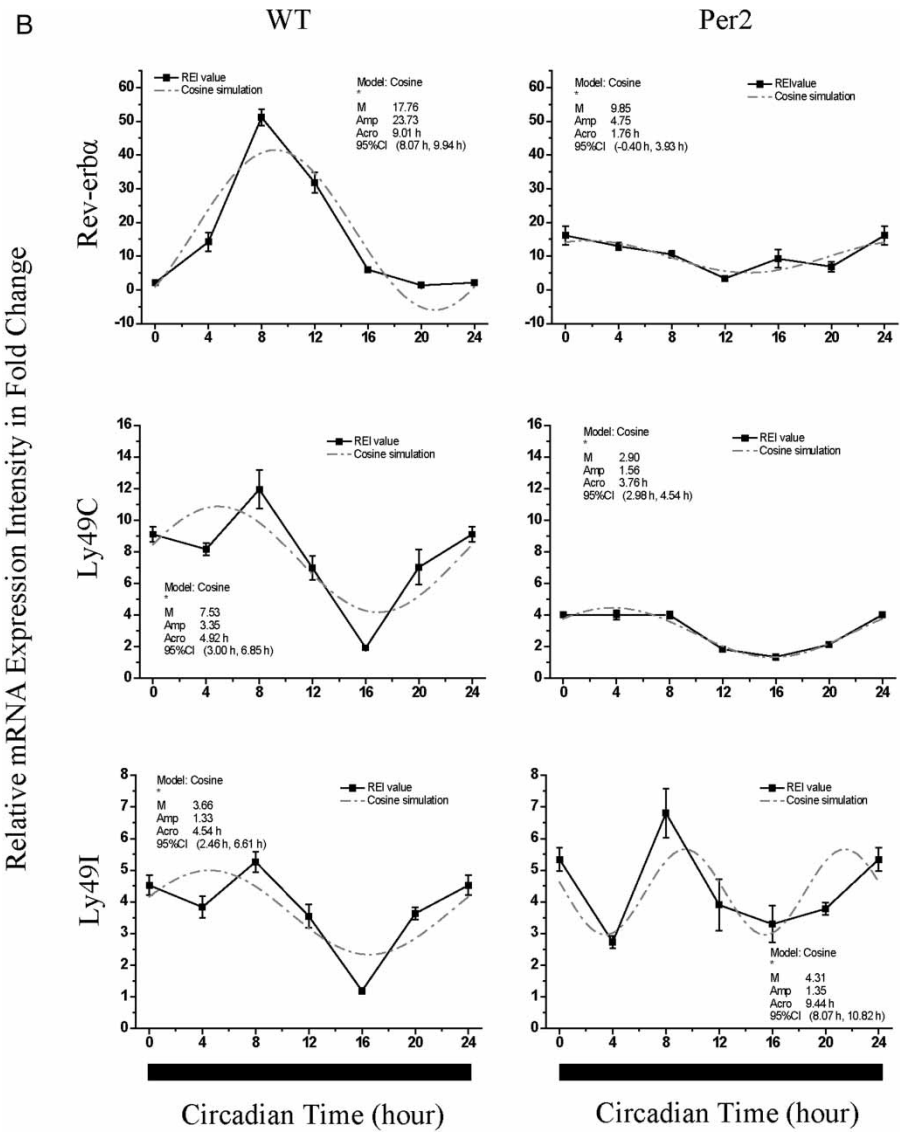

FIGURE 6 Continued

Discussion

In this study, we employed four different aspects (genotypes: WT and *mPer2*$^{-/-}$; lighting conditions: light/dark (LD) and dark/dark (DD)) to systematically analyze the circadian expression profiles of several key genes involved in cytotoxicity and INF-γ production in mice bone marrow. The overall mRNA expression levels of *Ly49C*, *Ly49I*, and *Nkg2d* were significantly downregulated in *mPer2*$^{-/-}$ mice (see Figure 2).

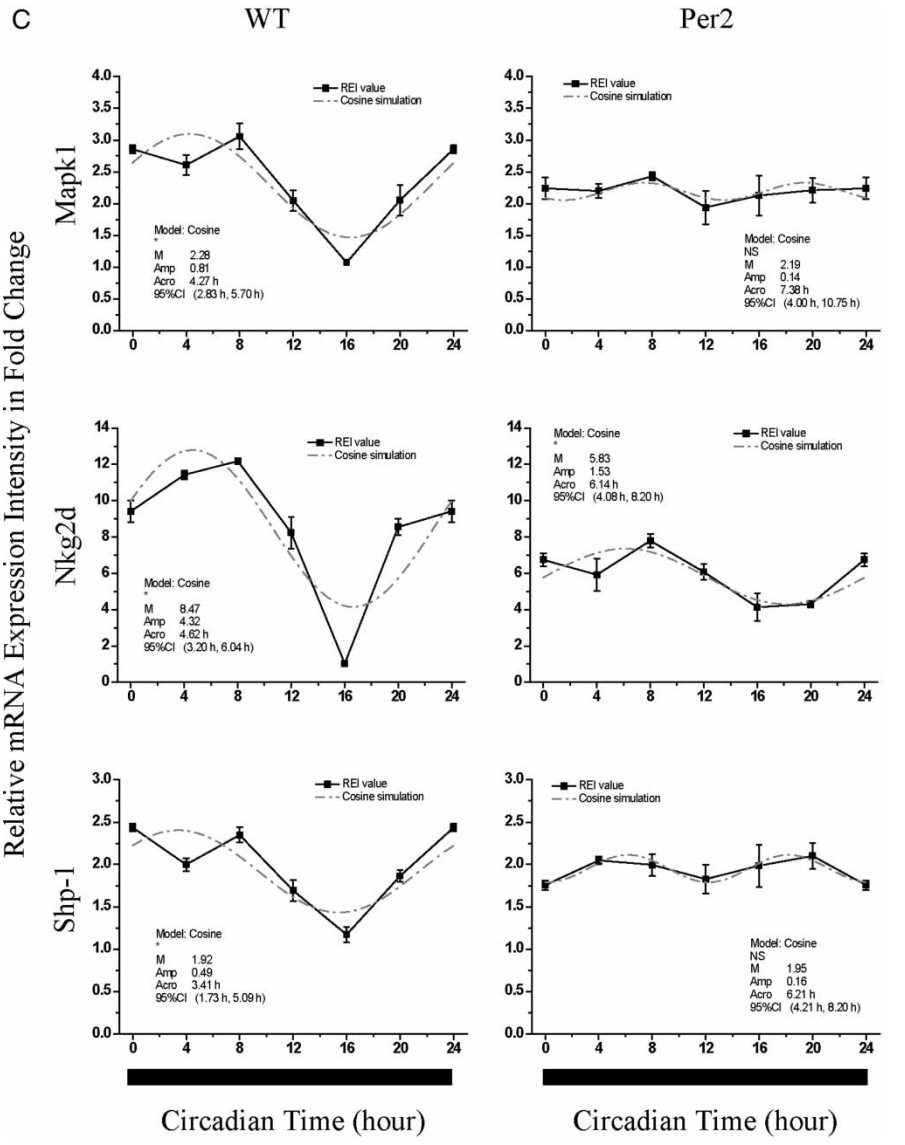

FIGURE 6 Continued

Furthermore, circadian expression profiling showed that *Ly49C* and *Nkg2d* exhibited 24 h oscillations in WT mice under LD and DD. However, these rhythmic expressions were disrupted in *mPer2*$^{-/-}$ mice (see Figures 3 and 6). Additionally, and consistent with previous studies (Chen et al., 2000; Tsinkalovsky et al., 2006), robust circadian oscillations in mRNA levels of *mPer1* and *mRev-erbα* were observed in the bone marrow of WT mice entrained to LD and DD conditions. The disrupted oscillatory expression of these three clock genes in *mPer2*$^{-/-}$ mice bone

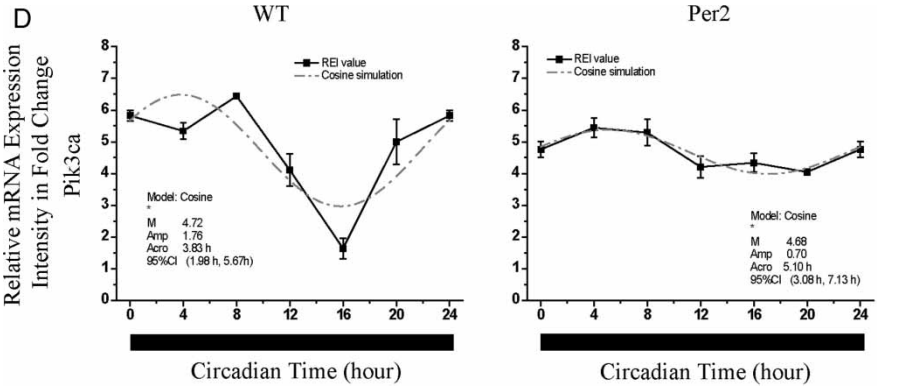

FIGURE 6 Continued

marrow is shown in Figures 3 and 6. To our knowledge, this is the first report of the circadian characteristics of *Ly49C* and *Nkg2d* in mice. In addition, the association of *mPer2* knockout with the downregulation in *Ly49C* and *Nkg2d* expressions indicates that these two critical cytotoxicity regulation receptors probably play an important role in mediating *mPer2* regulation of innate immune functions, cytotoxic response, and IFN-γ production (Pende et al., 2001). *Pik3ca* is well known for its important role in carcinogenesis and cytotoxicity regulation. Mutation or overexpression of this kinase is associated with tumorigenesis (Jia et al., 2008).

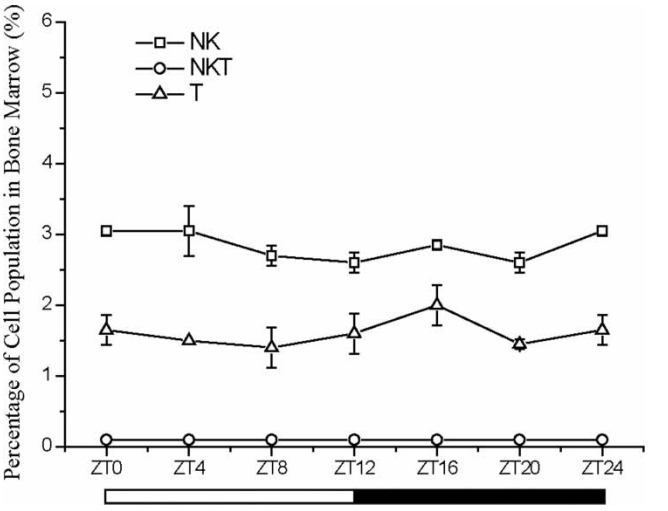

FIGURE 7 Daily variations of NK, NKT, and T cell numbers in bone marrow. Bone marrow from mice (n = 6/timepoint) for six timepoints during the day (ZT 0, 4, 8, 12, 16, and 20) were labeled with antibodies. The NK, NKT, and T cell populations were determined by flow cytometry. The percentage of cell population for NK (□), NKT (○), and T cells (△) is plotted as mean ± SD.

Although the overall expression level of *Pik3ca* is similar in WT and *mPer2*$^{-/-}$ mice, the expression levels of this kinase appear to be much higher in DD than in LD with a large amplitude in WT mice, whereas in *mPer2*$^{-/-}$ mice the amplitude is comparable to LD animals (see Figures 3 and 6). Taken together, these results implicate an important role of *mPer2* in regulating the expression of cytotoxicity regulators.

In order to characterize the cyclical variation in gene expression with time, Fourier "linear" regression analysis was performed using two commonly used models: circadian (24 h) and circasemidian (12 h). These two models had been shown to be suitable for most diurnal cycles (Fernandez et al., 2003). However, when applied to explore the cycling of gene expression with a period between circasemidian and circadian, more models are needed in order to accurately match the data. In the present study, although a significant circasemidian cycle was documented for *Bmal1* and *Pik3ca* in LD WT mice, *Ly49I* in Per2 LD mice (see Figure 3), and *Bmal1* and *Ly49I* in DD Per2 mice (see Figure 6), it did not accurately represent the time series data. Varied *Bmal1* expression in mice bone marrow had been reported previously (Granda et al., 2005). Thus, we performed a more complete regression analysis using a series of models differing in period by 1 h within a window of periods of 12 to 24 h. With this approach, a significant 22 h cycle for *Bmal1* ($p = 0.030$) and 21 h cycle for *Pik3ca* ($p = 0.036$) in LD WT mice were detected (see Table 4), which are close to being circadian in period. A significant 20 h cycle for Bmal1 ($p = 0.037$) in DD *mPer2*$^{-/-}$ mice was detected as well. However, it varies in anti-phase compared to that in DD WT mice (see Figure 6

TABLE 4 Post-cosine regression analysis for significant circasemidian cyclic expressed genes

	p value for CRA				
CRA model	Bmal1/LD/WT[a]	Pik3ca/LD/WT	Ly49I/LD/Per2	Bmal1/DD/Per2[b]	Ly49I/DD/Per2
12 h	0.00321	0.02735	0.03701	0.02161	0.03182
13 h	0.00146	0.00892	0.10961	0.03524	0.02480
14 h	0.00086	0.00633	0.25833	0.02866	0.03422
15 h	0.00045	0.00828	0.49065	0.02083	0.07288
16 h	0.00024	0.01113	0.76219	0.01761	0.14598
17 h	0.00020	0.01301	0.96330	0.01780	0.23411
18 h	0.00035	0.01474	0.98266	0.02089	0.31073
19 h	0.00107	0.01814	0.82521	0.02722	0.36377
20 h	0.00383	0.02488	0.60279	0.03716	0.39554
21 h	0.01204	0.03631	0.41080	0.05058	0.41355
22 h	0.03027	0.05324	0.27722	0.06658	0.42426
22 h	0.06128	0.07556	0.19234	0.08389	0.43154
22 h	0.10407	0.10233	0.13959	0.10133	0.43727

[a] Expression of Bmall in LD WT Mice
[b] Expression of Bmall in DD mPer2 Knockout Mice

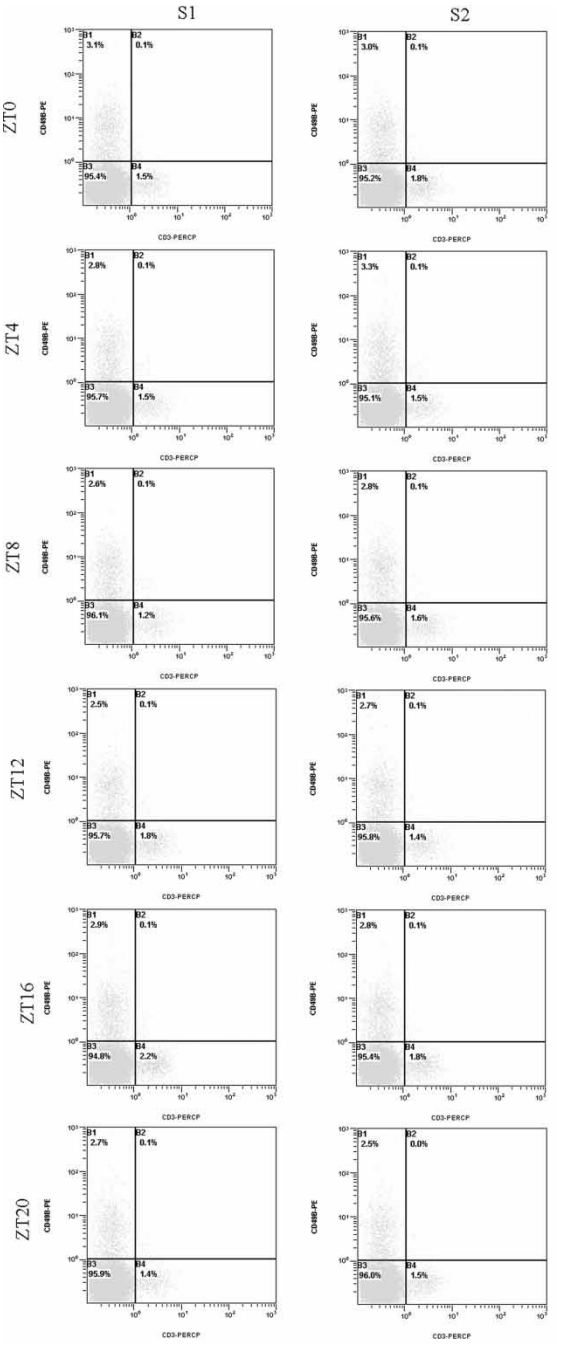

FIGURE 8 FACS analysis of NK, NKT, and T cell populations in bone marrow. Bone marrow from mice (n = 6/timepoint) of six timepoints during the day (ZT 0, 4, 8, 12, 16, and 20) were labeled with antibodies (CD9B-PE and CD3-PERCP). At each timepoint, six mice were randomly grouped into two individual groups and applied to FACS analysis (encoded as S1 and S2).

and Table 4). Thus, it is suggested that carrying out a more complete cosine analysis is necessary to obtain the most accurate regression model.

Bone marrow is the source of hematopoietic stem cells (HSC) that give rise to leukocytes and cells of the immune system that defend the body against infectious diseases (Freud et al., 2006; Trigg, 2004). Activation of these immune cells is necessary for host defenses against intracellular pathogens infections, destroying infected or transformed cells, and mediating tumor surveillance (Biron et al., 1989; Trinchieri, 1989). Cell-surface expressed receptors that trigger the activation of NK, NKT, and other T lymphocyte cells can be categorized into two functional types: inhibitory and stimulatory (Lanier, 1997). The lectin-like NKG2D molecule constitutes one set of stimulatory receptors. Many studies suggest that NKG2D may directly activate or co-stimulate cytolytic killing processes and release of cytokines, such as IFN-γ from NK, NKT, and T cells (Ho et al., 2002; Pende et al., 2001). Cell surface expression of NKG2D has been found in all NK cells, most $NK1.1^+$ T cells, and some γδ T cells, activated $CD8^+$ αβ T cells, partial $CD4^+$ αβ T cells, and activated macrophages (Raulet, 2003). All of these leukocytes are originated from bone marrow. In the present study, we observed mRNA expression and circadian fluctuation of *Nkg2d* in mouse bone marrow, whereas its circadian expression was significantly disrupted and downregulated in $mPer2^{-/-}$ mice (see Figures 3 and 6). This circadian expression was not due to the variation of NK, NKT, or T cell numbers in bone marrow during the day (see Figures 7 and 8). Besides, circadian oscillation of *Nkg2d* had been observed in the spleen of WT mice (data not shown). All of these suggest that the defects observed in innate immunity and cancer surveillance in $mPer2^{-/-}$ mice are likely associated with the deficiency of this immune activation gene (Fu et al., 2002; Liu et al., 2006).

However, repression in expression of another two NK, NKT, and T-cell activation inhibitory receptors, *Ly49C* and *Ly49I*, was observed in $mPer2^{-/-}$ mice in LD (see Figures 3 and 5) and *Ly49C* in DD (see Figures 5 and 6). These inhibitory receptors repress cellular cytotoxicity processes by recruiting SHP phosphatase and attenuating intracellular signals (Burshtyn et al., 1996; Mason et al., 1997). Theoretically, reduction in the expression of inhibitory receptors should lead to prolonged and enhanced cytotoxic signals. However, reduction in cytotoxicity and IFN-γ production in $mPer2^{-/-}$ mice was observed when they were subjected to endotoxic shock in a previous study (Liu et al., 2006), which may be related to reduction in expression of the activating receptor *Nkg2d* in the present study. Further investigation is needed to clarify the mechanisms regulating these genes.

Circadian oscillations in the mRNA and protein level of IFN-γ have been reported in rats and mice (Arjona et al., 2005, 2006). It is suggested

that *mPer2* plays a regulatory role in the daily rhythm of IFN-γ production (Arjona et al., 2006). However, whether IFN-γ expression is directly regulated by the molecular circadian clock components of BMAL1/CLOCK is still unclear. Although putative E-box binding sites were predicted in the IFN-γ gene promoter, to our knowledge no one has reported BMAL1/CLOCK binding to them. Another possibility is that clock-controlled IFN-γ expression is achieved indirectly (i.e., BMAL1/CLOCK modulates the circadian expression of some key components, and these components in turn trigger the circadian production of IFN-γ). Regulation of IFN-γ production is surely a relatively more complex process. It could be hormonal or regulated via gene-mediated pathways. Previously, we found a time-dependent induction of IFN-γ to LPS-induced endotoxic shock during the day, and the induction level of IFN-γ to LPS in *mPer2*$^{-/-}$ mice was significantly downregulated (Liu et al., 2006). In one of our unpublished studies, we found that the circadian regulation of IFN-γ induction was closely correlated with serum corticosterone induction. This indicates that the circadian regulation of IFN-γ expression can be due to circadian regulation of hormones. We demonstrated in this study that the circadian regulation of cytotoxicity and IFN-γ production could also been achieved by circadian regulation of *Ly49C*, *Ly49I*, and *Nkg2d*.

Although *mPer2* acts as an indispensable component in mammalian circadian maintenance by negatively inhibiting its own transcription, loss of *mPer2* function is associated with downregulation in the expression of many other genes, especially those involved in innate immune regulation, cell cycle regulation, and tumor suppression, such as *c-Myc*, *Cyclin D1*, *Cyclin A*, *Mdm-2*, and *Gadd45α* (Lee, 2006). Another investigation showed that over-expression of *mPer2* could upregulate *p53* and *bax* expression in Lewis lung carcinoma cells (Hua et al., 2006). This indicates that mPer2 could positively regulate gene expression but negatively modulate molecular circadian clocks. A growing body of investigations has indicated that *mPer2* exhibits a positive effect on the expression of IFN-γ. At some timepoints during the day, IFN-γ serum and splenic levels in *mPer2* mutant mice are significantly lower than those in WT mice (Arjona et al., 2006). Even under stress conditions, induction of IFN-γ to LPS challenge is significantly downregulated in *mPer2* mutant mice (Liu et al., 2006). In the present study, we also demonstrated that the expression of *Ly49C*, *Ly49I*, and *Nkg2d* involved in cytotoxicity and IFN-γ production regulation is downregulated in *mPer2*$^{-/-}$ mice.

In mammals, about 2–10% of genes have been reported to be clock-controlled genes (CCG) (Panda et al., 2002; Storch et al., 2002). A well-established model of transcriptional regulation of CCGs by clock components is achieved via positive transcriptional activation by BMAL1/CLOCK and negatively regulated by PER (Ko et al., 2006). In the

present study, loss of *mPer2* function did not show too much of an effect on the expression of *mBmal1* and *mClock* in mice bone marrow, except for upregulated *Bmal1* expression in DD mPer2$^{-/-}$ mice. This suggests the regulation of *Ly49C* and *Nkg2d* by *mPer2* is probably not through the traditional transcriptional-translational feedback loops. However, in order to elucidate the details of how *mPer2* manages the transcription of these three genes (directly or indirectly), more evidence is needed.

In conclusion, our data suggest the circadian oscillation of *Ly49C* and *Nkg2d* is regulated by *mPer2* in mice bone marrow. These two genes encode two key receptors that modulate the host immune defense, cytotoxic response, and IFN-γ production. As a result, the deregulation of these three genes in *mPer2*$^{-/-}$ mice bone marrow may help to explain the inhibition of acute inflammation response and inflammatory cytokines release to endotoxic shock. The disruption of the circadian rhythm in *mPer2*$^{-/-}$ mice bone marrow also indicates the deficiency observed in IFN-γ production in *mPer2*$^{-/-}$ mice is developmentally defective in related gene functions (Liu et al., 2006).

ACKNOWLEDGMENTS

This project is supported by National Natural Science Foundation of China (30770786) and National Natural Science Foundation of China (30628023). We wish to thank Yang Li (Institute of Psychology, CAS) for taking care of the mice and Kai Wang (Aarhus University, DK) for helpful statistical assistance.

The authors report no conflicts of interest. The authors alone are responsible for the content and writing of the paper.

REFERENCES

Albrecht U, Sun ZS, Eichele G, Lee CC. (1997). A differential response of two putative mammalian circadian regulators, mper1 and mper2, to light. *Cell* 91:1055–1064.

Arjona A, Sarkar DK. (2005). Circadian oscillations of clock genes, cytolytic factors, and cytokines in rat NK cells. *J. Immunol.* 174:7618–7624.

Arjona A, Sarkar DK. (2006). The circadian gene mPer2 regulates the daily rhythm of IFN-gamma. *J. Interferon Cytokine Res.* 26:645–649.

Billadeau DD, Upshaw JL, Schoon RA, Dick CJ, Leibson PJ. (2003). NKG2D-DAP10 triggers human NK cell-mediated killing via a Syk-independent regulatory pathway. *Nat. Immunol.* 4:557–564.

Biron CA, Byron KS, Sullivan JL. (1989). Severe herpes virus infections in an adolescent without natural killer cells. *N. Engl. J. Med.* 320:1731–1735.

Bittman EL, Doherty L, Huang L, Paroskie A. (2003). Period gene expression in mouse endocrine tissues. *Am. J. Physiol. Regul. Integr. Comp. Physiol.* 285:R561–R569.

Boivin DB, James FO, Wu A, Cho-Park PF, Xiong H, Sun ZS. (2003). Circadian clock genes oscillate in human peripheral blood mononuclear cells. *Blood* 102:4143–4145.

Burshtyn DN, Scharenberg AM, Wagtmann N, Rajagopalan S, Berrada K, Yi T, Kinet JP, Long EO. (1996). Recruitment of tyrosine phosphatase HCP by the killer cell inhibitor receptor. *Immunity* 4:77–85.

Chen YG, Mantalaris A, Bourne P, Keng P, Wu JH. (2000). Expression of mPer1 and mPer2, two mammalian clock genes, in murine bone marrow. *Biochem. Biophys. Res. Commun.* 276:724–728.

Dardente H, Cermakian N. (2007). Molecular circadian rhythms in central and peripheral clocks in mammals. *Chronobiol. Int.* 24:195–213.

Dimasi N, Biassoni R. (2005). Structural and functional aspects of the Ly49 natural killer cell receptors. *Immunol. Cell Biol.* 83:1–8.

Fernandez JR, Mojon A, Hermida RC, Alonso I. (2003). Methods for comparison of parameters from longitudinal rhythmometric models with multiple components. *Chronobiol. Int.* 20:495–513.

Freud AG, Caligiuri MA. (2006). Human natural killer cell development. *Immunol. Rev.* 214:56–72.

Fu L, Pelicano H, Liu J, Huang P, Lee C. (2002). The circadian gene Period2 plays an important role in tumor suppression and DNA damage response in vivo. *Cell* 111:41–50.

Graham DB, Cella M, Giurisato E, Fujikawa K, Miletic AV, Kloeppel T, Brim K, Takai T, Shaw AS, Colonna M, Swat W. (2006). Vav1 controls DAP10-mediated natural cytotoxicity by regulating actin and microtubule dynamics. *J. Immunol.* 177:2349–2355.

Granda TG, Liu XH, Smaaland R, Cermakian N, Filipski E, Sassone-Corsi P, Levi F. (2005). Circadian regulation of cell cycle and apoptosis proteins in mouse bone marrow and tumor. *FASEB J.* 19:304–306.

Ho EL, Carayannopoulos LN, Poursine-Laurent J, Kinder J, Plougastel B, Smith HR, Yokoyama WM. (2002). Costimulation of multiple NK cell activation receptors by NKG2D. *J. Immunol.* 169:3667–3675.

Hua H, Wang Y, Wan C, Liu Y, Zhu B, Yang C, Wang X, Wang Z, Cornelissen-Guillaume G, Halberg F. (2006). Circadian gene mPer2 overexpression induces cancer cell apoptosis. *Cancer Sci.* 97:589–596.

James FO, Boivin DB, Charbonneau S, Belanger V, Cermakian N. (2007). Expression of clock genes in human peripheral blood mononuclear cells throughout the sleep/wake and circadian cycles. *Chronobiol. Int.* 24:1009–1034.

Jamieson AM, Diefenbach A, McMahon CW, Xiong N, Carlyle JR, Raulet DH. (2002). The role of the NKG2D immunoreceptor in immune cell activation and natural killing. *Immunity* 17:19–29.

Jia S, Liu Z, Zhang S, Liu P, Zhang L, Lee SH, Zhang J, Signoretti S, Loda M, Roberts TM, Zhao JJ. (2008). Essential roles of PI(3)K-p110beta in cell growth, metabolism and tumorigenesis. *Nature* 454:776–779.

Jin X, Shearman LP, Weaver DR, Zylka MJ, de Vries GJ, Reppert SM. (1999). A molecular mechanism regulating rhythmic output from the suprachiasmatic circadian clock. *Cell* 96:57–68.

Jud C, Schmutz I, Hampp G, Oster H, Albrecht U. (2005). A guideline for analyzing circadian wheel-running behavior in rodents under different lighting conditions. *Biol. Proced. Online* 7:101–116.

Ko CH, Takahashi JS. (2006). Molecular components of the mammalian circadian clock. *Hum. Mol. Genet.* 15 (Spec. No. 2):R271–R277.

Lanier LL. (1997). Natural killer cells: From no receptors to too many. *Immunity* 6:371–378.

Lee CC. (2006). Tumor suppression by the mammalian Period genes. *Cancer Causes Control* 17:525–530.

Liu J, Malkani G, Shi X, Meyer M, Cunningham-Runddles S, Ma X, Sun ZS. (2006). The circadian clock Period 2 gene regulates gamma interferon production of NK cells in host response to lipopolysaccharide-induced endotoxic shock. *Infect. Immun.* 74:4750–4756.

Liu S, Cai Y, Sothern RB, Guan Y, Chan P. (2007). Chronobiological analysis of circadian patterns in transcription of seven key clock genes in six peripheral tissues in mice. *Chronobiol. Int.* 24:793–820.

Mason LH, Gosselin P, Anderson SK, Fogler WE, Ortaldo JR, McVicar DW. (1997). Differential tyrosine phosphorylation of inhibitory versus activating Ly-49 receptor proteins and their recruitment of SHP-1 phosphatase. *J. Immunol.* 159:4187–4196.

Mendez-Ferrer S, Lucas D, Battista M, Frenette PS. (2008). Haematopoietic stem cell release is regulated by circadian oscillations. *Nature* 452:442–447.

Nelson W, Tong YL, Lee JK, Halberg F. (1979). Methods for cosinor-rhythmometry. *Chronobiologia* 6:305–323.

Panda S, Antoch MP, Miller BH, Su AI, Schook AB, Straume M, Schultz PG, Kay SA, Takahashi JS, Hogenesch JB. (2002). Coordinated transcription of key pathways in the mouse by the circadian clock. *Cell* 109:307–320.

Pende D, Cantoni C, Rivera P, Vitale M, Castriconi R, Marcenaro S, Nanni M, Biassoni R, Bottino C, Moretta A, Moretta L. (2001). Role of NKG2D in tumor cell lysis mediated by human NK cells: Cooperation with natural cytotoxicity receptors and capability of recognizing tumors of nonepithelial origin. *Eur. J. Immunol.* 31:1076–1086.

Portaluppi F, Touitou Y, Smolensky MH. (2008). Ethical and methodological standards for laboratory and medical biological rhythm research. *Chronobiol. Int.* 25:999–1016.

Raulet DH. (2003). Roles of the NKG2D immunoreceptor and its ligands. *Nat. Rev. Immunol.* 3:781–790.

Reppert SM, Weaver DR. (2002). Coordination of circadian timing in mammals. *Nature* 418:935–941.

Sasaki S, Tagawa Y, Iwakura Y, Nakane A. (2006). The role of gamma interferon in acquired host resistance against *Staphylococcus aureus* infection in mice. *FEMS Immunol. Med. Microbiol.* 46:367–374.

Stolwijk AM, Straatman H, Zielhuis GA. (1999). Studying seasonality by using sine and cosine functions in regression analysis. *J. Epidemiol. Community Health* 53:235–238.

Storch KF, Lipan O, Leykin I, Viswanathan N, Davis FC, Wong WH, Weitz CJ. (2002). Extensive and divergent circadian gene expression in liver and heart. *Nature* 417:78–83.

Trigg ME. (2004). Hematopoietic stem cells. *Pediatrics* 113:1051–1057.

Trinchieri G. (1989). Biology of natural killer cells. *Adv. Immunol.* 47:187–376.

Tsinkalovsky O, Filipski E, Rosenlund B, Sothern RB, Eiken HG, Wu MW, Claustrat B, Bayer J, Levi F, Laerum OD. (2006). Circadian expression of clock genes in purified hematopoietic stem cells is developmentally regulated in mouse bone marrow. *Exp. Hematol.* 34:1249–1261.

Wall L, Burke F, Barton C, Smyth J, Balkwill F. (2003). IFN-gamma induces apoptosis in ovarian cancer cells in vivo and in vitro. *Clin. Cancer Res.* 9:2487–2496.